A MATHEMATICAL STUDY OF NERVE FIBER INTERACTION

JOHN W. CLARK *and* ROBERT PLONSEY

From the Bioengineering Group, Electrical Engineering Department, Rice University, Houston, Texas 77001 and the Biomedical Engineering Department, Case Western Reserve University, Cleveland, Ohio 44106

ABSTRACT This paper presents a quantitative description of the electric field interaction between two adjacent unmyelinated nerve fibers (one active, the other inactive) for the infinite medium and nerve trunk geometries, and considers their dependence on various electrical and geometrical parameters. Based on the use of synthetic giant axon data, the conclusion of this study is that the cross-sectional area of the nerve trunk and the specific resistivity of the interstitial medium are of particular importance to the degree of fiber interaction. Other factors such as separation distance between fibers, axoplasmic resistivity, membrane resistance, and capacitance of the inactive fiber, are also investigated and found to be of secondary importance.

INTRODUCTION

Bioelectric field interaction between adjacent nerve fibers has been a topic of interest in the area of electrophysiology for a number of years.[1] This paper presents a quantitative description of the induced transmembrane potential produced in the inactive fiber due to activity in the adjacent active fiber, for the infinite medium and nerve trunk geometries, and considers their dependence on electrical and geometrical parameters. Since consideration of two fibers represents the simplest example for study of interaction, this problem might be characterized as the "basic" model.

Mathematical expressions for potential in the axoplasmic and extracellular media of the single active nerve fiber situated in an extensive volume conductor have been developed (Clark and Plonsey, 1966 and 1968). These potentials are given as:

$$\Phi^o(\rho_a, z) = \tfrac{1}{2}\pi \int_{-\infty}^{\infty} \frac{F_m(k)K_0(|k|\rho_a)e^{-jkz}}{\alpha(|k|a_a)K_0(|k|a_a)}\,dk \qquad (1)$$

$$\Phi^i(\rho_a, z) = \tfrac{1}{2}\pi \int_{-\infty}^{\infty} \frac{F_m(k)I_0(|k|\rho_a)e^{-jkz}}{\beta(|k|a_a)I_0(|k|a_a)}\,dk \qquad (2)$$

where $F_m(k)$ is the Fourier transform of the transmembrane potential distribution

[1] Katz and Schmitt (1940, 1942); Arvanitaki (1942); Marrazzi and Lorente de Nó (1944); Granit et al. (1944); Grundfest and Magnes (1951); Konishi (1955); Esplin (1962); Bures et al. (1967).

$\Phi_m(z)$ given as:

$$\Phi_m(z) = \Phi_s^i(z) - \Phi_s^o(z), \tag{3}$$

(where Φ_s^i and Φ_s^o are the inner and outer membrane surface potential distributions, respectively) and $\alpha(|\ k\ |a_s)$ and $\beta(|\ k\ |a_s)$ are defined as:

$$\alpha(|\ k\ |\ a_s) = -\left[\frac{\sigma_0}{\sigma_{is}} \frac{K_1(|\ k\ |\ a_s)I_0(|\ k\ |\ a_s)}{K_0(|\ k\ |\ a_s)I_1(|\ k\ |\ a_s)} + 1\right] \tag{4}$$

$$\beta(|\ k\ |\ a_s) = \left[\frac{\sigma_{is}}{\sigma_0} \frac{I_1(|\ k\ |\ a_s)K_0(|\ k\ |\ a_s)}{I_0(|\ k\ |\ a_s)K_1(|\ k\ |\ a_s)} + 1\right]. \tag{5}$$

Here, K_0 and K_1 are modified Bessel functions of the second kind, orders 0 and 1, respectively, while, I_0 and I_1 are modified Bessel functions of the first kind, orders 0 and 1. The terms σ_0 and σ_{is} represent the specific conductivities (mho/cm) of the extracellular and axoplasmic media of the active nerve fiber and the term a_s represents the radius of the fiber in centimeters.

The transmembrane potential distribution is approximated mathematically as the sum of three gaussian distributions as described in Clark and Plonsey (1966), p. 103. That is,

$$\Phi_m(z) = \sum_{i=1}^{3} A_i e^{B^2_i(z-c_i)^2}. \tag{6}$$

The Fourier transform $F_m(k)$ of this potential distribution is defined as:

$$F_m(k) = \int_{-\infty}^{\infty} \Phi_m(z) e^{jkz}\, dz \tag{7}$$

and upon substitution of equation 6 into equation 7, it is easily evaluated as:

$$F_m(k) = \sqrt{\pi} \sum_{i=1}^{3} \frac{A_i}{B_i} e^{-k^2/4B^2_i} e^{jkc_i}. \tag{8}$$

Upon substitution of equation 8 into equations 1 and 2, one obtains the following equations for potential in the extra- and intracellular media of the single fiber *in situ*.

$$\Phi^o(\rho_s, \theta, z) = \frac{1}{2\sqrt{\pi}} \int_{-\infty}^{\infty} \sum_{i=1}^{3} \frac{A_i}{B_i} \frac{K_0(|\ k\ |\ \rho_s)e^{-k^2/4B_i^2}}{\alpha(|\ k\ |\ a_s)K_0(|\ k\ |\ a_s)} e^{jk(z-c_i)}\, dk \tag{9}$$

$$\Phi^i(\rho_s, \theta, z) = \frac{1}{2\sqrt{\pi}} \int_{-\infty}^{\infty} \sum_{i=1}^{3} \frac{A_i}{B_i} \frac{I_0(|\ k\ |\ \rho_s)e^{-k^2/4B_i^2}}{\beta(|\ k\ |\ a_s)I_0(|\ k\ |\ a_s)} e^{jk(z-c_i)}\, dk. \tag{10}$$

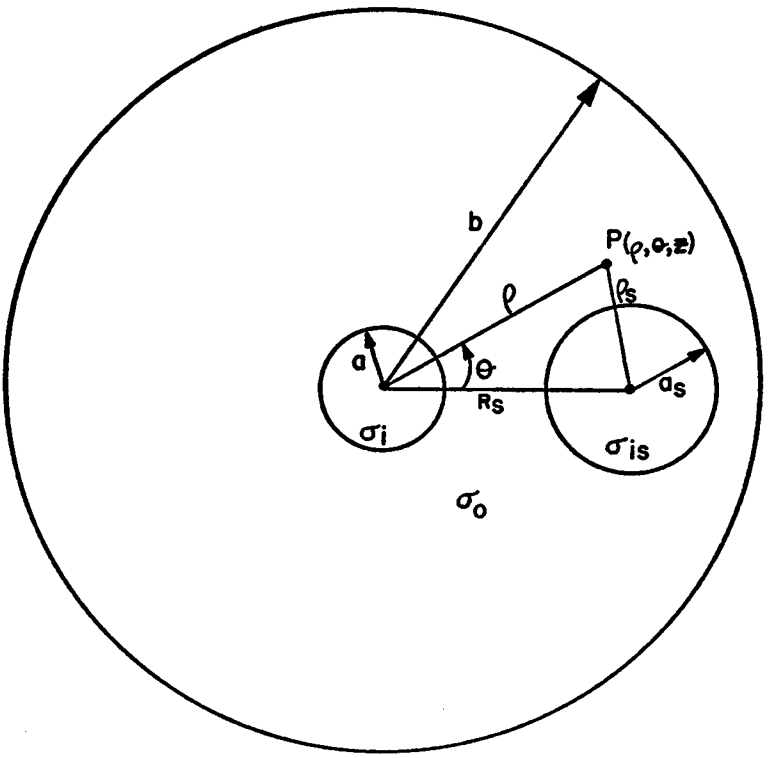

FIGURE 1 Geometry of the fiber interaction problem.

Mathematical Formulation of the Interaction Problem

In this study we consider a nerve trunk containing two parallel, unmyelinated nerve fibers, one active, the other inactive (Fig. 1). The interstitial medium of the trunk is considered to possess an average specific conductivity σ_0 ,[2] while the axoplasmic conductivities of the inactive and active fibers are σ_i and σ_{is} respectively. The nerve trunk is further assumed to lie in a bathing medium of essentially infinite extent, possessing a specific conductivity σ_e . (These specific conductivities are all given in units of millimhos per centimeter.) In addition, the membrane of the inactive fiber is characterized electrically as a distributed parallel resistance-capacitance network. As such, the inactive fiber membrane is characterized by a specific conductivity per unit area $\bar{\sigma}_m$ and specific capacity per unit area $\bar{c}_m$. The epineural sheath of the nerve trunk is assumed to be essentially resistive in nature[3] and therefore may be characterized by the specific conductivity per unit area $\bar{\sigma}_{sh}$. The active fiber is located a

[2] This average conductivity σ_0 represents the conductivity of an interstitial medium containing interstitial fluid, inactive nerve fibers, and blood vessels.
[3] Clark (1967).

radial distance R_s from the center of the inactive fiber and the line joining their centers is chosen to be the horizontal axis ($\theta = 0°$). Referring to Fig. 1, the field point $P(\rho, \theta, z)$ is located a distance ρ_s from the center of the active source fiber, and a distance ρ from the center of the inactive fiber. The relationship between ρ, ρ_s, and R_s is given by the law of cosines.

$$\rho_s^2 = \rho^2 + R_s^2 - 2\rho R_s \cos\theta. \tag{11}$$

This model of fiber interaction in the nerve trunk is quite general in the sense that we may consider interaction in the infinite medium case as well by simply letting the nerve trunk radius (b) become large relative to the radial extent of the electric field of the source fiber.[4]

The general expression for potential in the axoplasmic region obtained as a solution to Laplace's equation in cylindrical coordinates under conditions of quasi-stationarity is:

$$\Phi^i(\rho, \theta, z) = \sum_{m=0}^{\infty} \cos n\theta \int_{-\infty}^{\infty} A_n(k) I_n(|\, k \,|\, \rho) e^{-jkz}\, dk, \tag{12}$$

where $I_n(|\, k \,|\, \rho)$ is the modified Bessel function of the first kind, order n, and the $A_n(k)$ are undetermined potential functions. The function I_n is chosen because it has both an appropriate behavior at $\rho \to 0$ and is linked to a desired complex exponential form in z.

The general expression for potential in the interstitial medium ($a \leq \rho \leq b$; but excluding the region occupied by the active fiber) is:

$$\Phi^o(\rho, \theta, z) = \Phi_s(\rho, \theta, z) + \sum_{n=0}^{\infty} \cos n\theta \int_{-\infty}^{\infty} [B_n(k) I_n(|\, k \,|\, \rho) + C_n(k) K_n(|\, k \,|\, \rho)] e^{-jkz}\, dk, \tag{13}$$

where $B_n(k)$ and $C_n(k)$ are undetermined potential functions, and I_n and K_n are the modified Bessel functions of the first and second kinds, respectively. The term $\Phi_s(\rho, \theta, z)$ in equation 13 represents the contribution of the active "source" fiber to the interstitial potential, while the second term, which is the general solution of Laplace's equation in the cylindrical medium ($a \leq \rho \leq b$), represents the perturbation effect of the inactive fiber and the sheath. One may also interpret this term as reflecting secondary sources that arise from conductivity discontinuities of inactive

[4] Previous work involving the potential distribution of a single active nerve fiber in a nerve trunk (Clark and Plonsey, 1968) indicates that letting the nerve trunk radius approach a factor of 50 times the active fiber radius is more than sufficient for the establishment of the infinite medium case. (The active "source" fiber considered in the study mentioned has the same electrical and geometrical characteristics as the active fiber of Fig. 1.)

fiber and sheath. According to Clark and Plonsey (1968), $\Phi_s(\rho, \theta, z)$ is given as:

$$\Phi_s(\rho, \theta, z) = \sum_{n=0}^{\infty} (2 - \delta_n^0) \cos n\theta \int_{-\infty}^{\infty} G(k) K_n(|k| R_s) I_n(|k| \rho) e^{-jkz}\, dk \quad \text{for} \quad \rho < R_s \tag{14}$$

$$\Phi_s(\rho, \theta, z) = \sum_{n=0}^{\infty} (2 - \delta_n^0) \cos \theta \int_{-\infty}^{\infty} G(k) I_n(|k| R_s) K_n(|k| \rho) e^{-jkz}\, dk \quad \text{for} \quad \rho > R_s, \tag{15}$$

where

$$G(k) \equiv \frac{F_m(k)}{2\pi\alpha(|k| a_s) K_0(|k| a_s)} \tag{16}$$

and

$$\delta_n^0 = 0 \quad \text{for} \quad n \neq 0 = 1 \quad \text{for} \quad n = 0. \tag{17}$$

While equations 14 and 15 are strictly valid for an active fiber in an infinite conducting medium it is assumed that the bioelectric sources responsible for Φ_s are not significantly affected by the inactive fiber and trunk sheath. In equation 16 the function $F_m(k)$ is the Fourier transform of the transmembrane potential distribution of the active fiber, and $\alpha(|k| a_s)$ is given by equation 4.

Substituting equations 14 and 15 into equation 13, one obtains

$$\Phi^o(\rho, \theta, z) = \sum_{n=0}^{\infty} \cos n\theta \int_{-\infty}^{\infty} [(P_n(k) + B_n(k)) I_n(|k| \rho) + C_n(k) K_n(|k| \rho)] e^{-jkz}\, dk \quad \text{for} \quad \rho < R_s \tag{18}$$

$$\Phi^o(\rho, \theta, z) = \sum_{n=0}^{\infty} \cos \theta \int_{-\infty}^{\infty} [B_n(k) I_n(|k| \rho) + (P_n(k) R_n(k) + C_n(k)) K_n(|k| \rho)] e^{-jkz}\, dk \quad \text{for} \quad \rho > R_s, \tag{19}$$

where:

$$P_n(k) \equiv (2 - \delta_n^0) G(k) K_n(|k| R_s) \tag{20}$$

$$R_n(k) \equiv I_n(|k| R_s) / K_n(|k| R_s). \tag{21}$$

The general expression for potential in the external medium is:

$$\Phi^e(\rho, \theta, z) = \sum_{n=0}^{\infty} \cos n\theta \int_{-\infty}^{\infty} D_n(k) K_n(|k| \rho) e^{-jkz}\, dk, \tag{22}$$

where $D_n(k)$ is the undetermined potential function and K_n is the modified Bessel function of the second kind, order n.

Boundary Conditions

The appropriate boundary conditions are the following.
At $\rho = a$:

(*a*) Current crossing the fiber membrane, assumed to be extremely thin, must be continuous. This condition is expressed mathematically as

$$-\sigma_i \frac{\partial \Phi^i}{\partial \rho}\bigg|_a = -\sigma_0 \frac{\partial \Phi^o}{\partial \rho}\bigg|_a = J_m(\theta, z), \tag{23}$$

where J_m is the transmembrane current density.

(*b*) The inactive fiber membrane is characterized electrically as a distributed parallel resistance-capacitance network. Corresponding to a transmembrane potential Φ_{mi} defined as

$$\Phi_{mi}(\theta, z) = \Phi^i(a, \theta, z) - \Phi^o(a, \theta, z), \tag{24}$$

one must have a transmembrane current density given by

$$J_m(\theta, z) = \bar{\sigma}_m \Phi_{mi}(\theta, z) + \bar{C}_m \frac{\partial \Phi_{mi}(\theta, z)}{\partial t}, \tag{25}$$

where $\bar{\sigma}_m$ is the specific conductivity and $\bar{C}_m$ is the specific capacity per unit area of the membrane.

The time derivative in equation 25 may be evaluated since we assume the existence of a propagated action potential in the negative z-direction, and therefore all field quantities vary as $(z + vt)$ where v is the propagation velocity. Thus, for a force field quantity $\psi(\rho, \theta, z)$, we have:

$$\psi(\rho, \theta, z, t) = \psi(\rho, \theta, (z + vt)) \tag{26}$$

and, consequently, as may be readily verified,

$$\frac{\partial \psi}{\partial t} = v \frac{\partial \psi}{\partial z}. \tag{27}$$

Thus, equation 25 becomes:

$$J_m(\theta, z) = \bar{\sigma}_m \Phi_m(\theta, z) + v\bar{C}_m \frac{\partial \Phi_m(\theta, z)}{\partial z}. \tag{28}$$

Thus, from equation 23, the appropriate boundary conditions to be applied at

$\rho = a$ are:

$$\sigma_i \frac{\partial \Phi^i}{\partial \rho}\bigg|_a + J_m = 0 \tag{29}$$

$$\sigma_0 \frac{\partial \Phi^o}{\partial \rho}\bigg|_a + J_m = 0 \tag{30}$$

where J_m is given by equation 28 and Φ_{mi} by equation 24.
At $\rho = b$:

Current crossing the connective tissue sheath is also assumed to be continuous. Thus

$$-\sigma_0 \frac{\partial \Phi^o}{\partial \rho}\bigg|_b = -\sigma_e \frac{\partial \Phi^e}{\partial \rho}\bigg|_b = J_{sh} \tag{31}$$

where J_{sh} is the trans-sheath current density. Since the sheath is considered to be essentially resistive in nature, J_{sh} may also be expressed as:

$$J_{sh} = \bar{\sigma}_{sh}\Phi_{sh}, \tag{32}$$

where $\bar{\sigma}_{sh}$ is the specific conductivity per unit area of the sheath and Φ_{sh} is the trans-sheath potential defined as:

$$\Phi_{sh}(\theta, z) = \Phi^o(b, \theta, z) - \Phi^e(b, \theta, z). \tag{33}$$

Therefore, from equation 31, the appropriate boundary conditions to be employed at $\rho = b$ are:

$$\sigma_0 \frac{\partial \Phi^o}{\partial \rho}\bigg|_b + J_{sh} = 0 \tag{34}$$

$$\sigma_e \frac{\partial \Phi^e}{\partial \rho}\bigg|_b + J_{sh} = 0, \tag{35}$$

where J_{sh} is given by equation 32 and Φ_{sh} by equation 33.

Utilizing the boundary condition equations 29, 30, 34, and 35, it is possible to solve for the unknown potential functions $A_n(k)$, $B_n(k)$, $C_n(k)$, and $D_n(k)$. When the expressions for these functions are found via simultaneous solution of the equations listed above, and subsequently substituted into equations 12, 18, 19, and 22, expressions for potential in the media of interest are obtained. These equations are listed in the Appendix.[5]

[5] See equations A 1–A 3.

Synthetic Data for Interaction Problem

Since the equations for potential listed in the Appendix are too complex to permit a general solution, we proceed by choosing a representative problem for which $\Phi_{mi}(z)$, the transmembrane potential distribution of the inactive fiber, and several other electrical and biometrical parameters, are available in the literature. The experiments of Watanabe and Grundfest (1961) on the crayfish lateral and medial giant axons of the ventral nerve cord provide a suitable example and the necessary data. The following values are chosen for the geometrical parameters of the model:

(1) $a_s = 60\ \mu$ (radius of source fiber);
(2) $a = 40\ \mu$ (radius of inactive fiber);
(3) $R_s = 160\ \mu$ (center to center distance between fibers).

The values chosen for the electrical parameters are:

(1) $\sigma_0 = 1/40$ mho/cm (specific conductivity of interstitial medium);
(2) $\sigma_i = \sigma_{is} = 1/94$ mho/cm (specific conductivity of axoplasmic media of inactive and source fibers);
(3) $\bar{C}_m = 0.61\ \mu F/cm^2$ (capacity per unit area of inactive fiber membrane);
(4) $\bar{\sigma}_m = 1/3100$ mho/cm^2 (conductivity per unit area of inactive fiber membrane);
(5) $\bar{\sigma}_m = 1/1000$ mho/cm^2 (conductivity per unit area of epineural sheath).

The values of the constants A_i, B_i, and C_i in equation 6 that result in a close fit to the monophasic action potential obtained from Watanabe and Grundfest are:[6]

$A_1 = 51.0$ mv	$B_1 = 8.0\ cm^{-1}$	$C_1 = 0.54$ cm
$A_2 = 72.0$ mv	$B_2 = 5.33\ cm^{-1}$	$C_2 = 0.66$ cm
$A_3 = 18.0$ mv	$B_3 = 3.33\ cm^{-1}$	$C_3 = 0.86$ cm.

The value for propagation velocity (v) obtained from Watanabe and Grundfest was 1000 cm/sec.

Approximations involved in the numerical evaluation of equations A 1–A 4 are essentially the same as those discussed in Clark and Plonsey (1966, 1968). The limits of integration employed in the numerical evaluation of these equations are (0, 0.24),

[6] These constants have the same values as were used in Clark and Plonsey (1968).

and these limits were obtained by evaluating and plotting the integrands of these equations so as to determine an upper bound on the variable of integration (y).

RESULTS

Numerical Evaluation of the External and Internal Potential Fields

The cross-sectional aspects of the computed potential field is shown in Fig. 2, where Φ^e appears as a function of ρ and θ in the plane $z = 0.5$ cm.[7] In observing this figure, one notes that the presence of the inactive fiber has a pronounced effect on the potential distribution in the interstitial medium of the nerve trunk. In the case of the single active nerve fiber in an extensive volume conductor, the equipotential lines of the extracellular field consist of concentric circles centered about the fiber. The distortion of the equipotential lines arises from both the inactive fiber and the sheath.

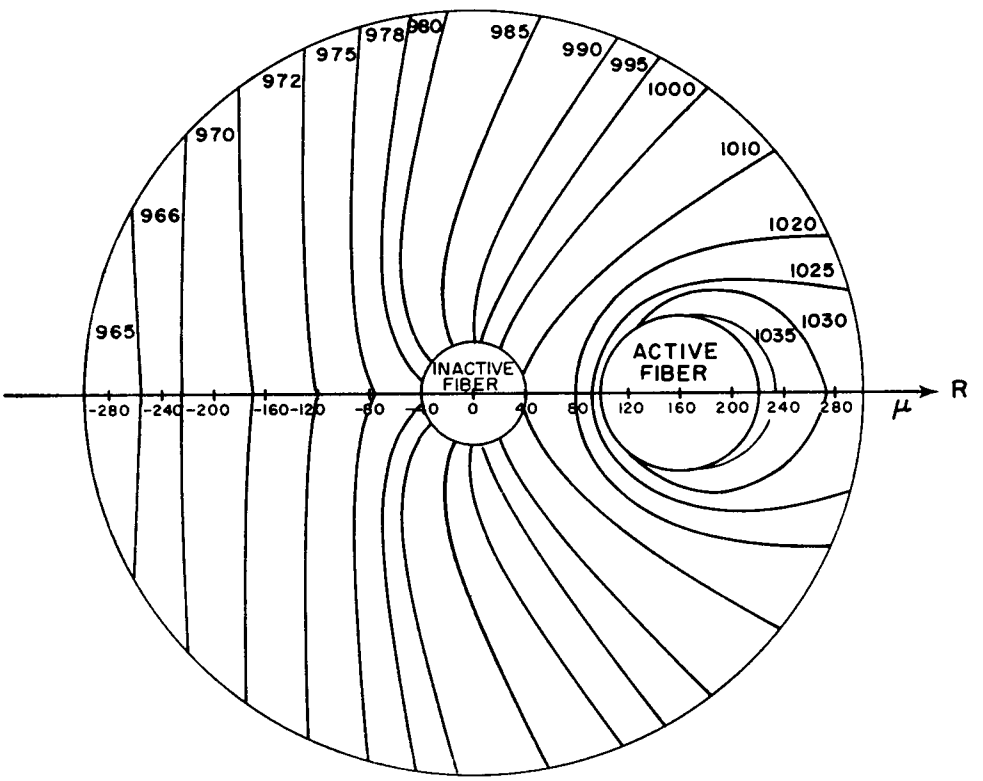

FIGURE 2 Cross-sectional aspect of the potential distribution within the interstitial medium, in the plane $z = 0.5$ cm.

[7] This plane was selected arbitrarily; a description of the longitudinal potential variation is given in Fig. 5 and is discussed later in this section.

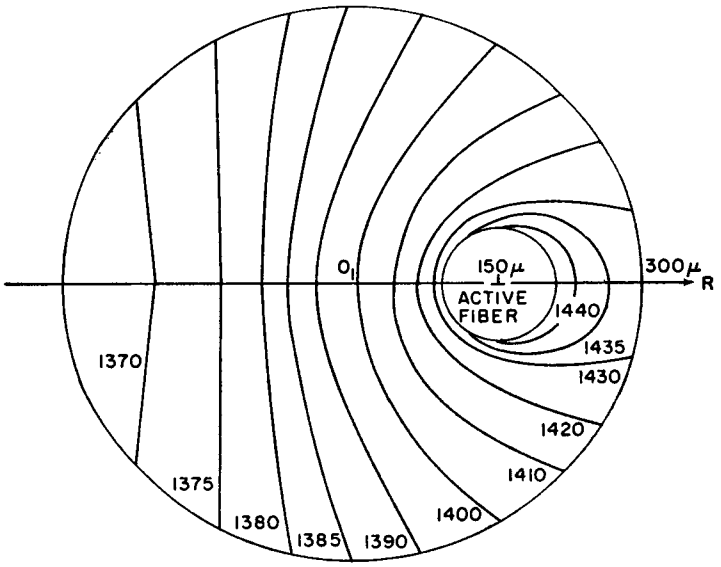

FIGURE 3 Cross-sectional aspect of the potential distribution in the interstitial medium of the nerve trunk containing a single active fiber. $z = 0.625$ cm (from Clark and Plonsey, 1968).

TABLE I

INTERNAL POTENTIAL Φ^i AT $z = 0.5$ cm AS A FUNCTION OF ρ AND θ (VALUES OF POTENTIAL IN μv)

θ	$\rho = 0.1\ \mu$	$\rho = 20\ \mu$	$\rho = 40\ \mu$
0°	−1189.211	−1189.360	−1189.694
30°	−1189.211	−1189.352	−1189.678
60°	−1189.209	−1189.330	−1189.634
90°	−1189.208	−1189.300	−1189.574
120°	−1189.207	−1189.270	−1189.514
150°	−1189.205	−1189.248	−1189.470
180°	−1189.205	−1189.240	−1189.454

The effect of the sheath alone is shown in Fig. 3 (taken from Clark and Plonsey, 1968). When, in addition, an inactive fiber is present within the interstitial medium of the trunk, further distortion of the field occurs, as in Fig. 2.

Computation of the internal potential Φ^i in the plane $z = 0.5$ cm reveals that for all practical purposes the axoplasmic medium of the initive fiber may be considered an isopotential region. For example, Table I indicates there is little variation in the magnitude of Φ^i with either radius (ρ) or angle (θ).

Since the value of Φ^i is approximately constant over the entire plane, one would expect from a consideration of Fig. 2 and the definition of the transmembrane potential that Φ_{mi} would vary as a function of angle θ. This is verified in Table II, where one

TABLE II

CALCULATED TRANSMEMBRANE POTENTIAL (Φ_{mi}) AS A FUNCTION OF ANGLE θ IN THE PLANE $z = 0.5$ cm

θ	Φ_m
Degree	μv
0	−181.835
30	−185.330
60	−191.894
90	−202.757
120	−210.094
150	−214.744
180	−216.303

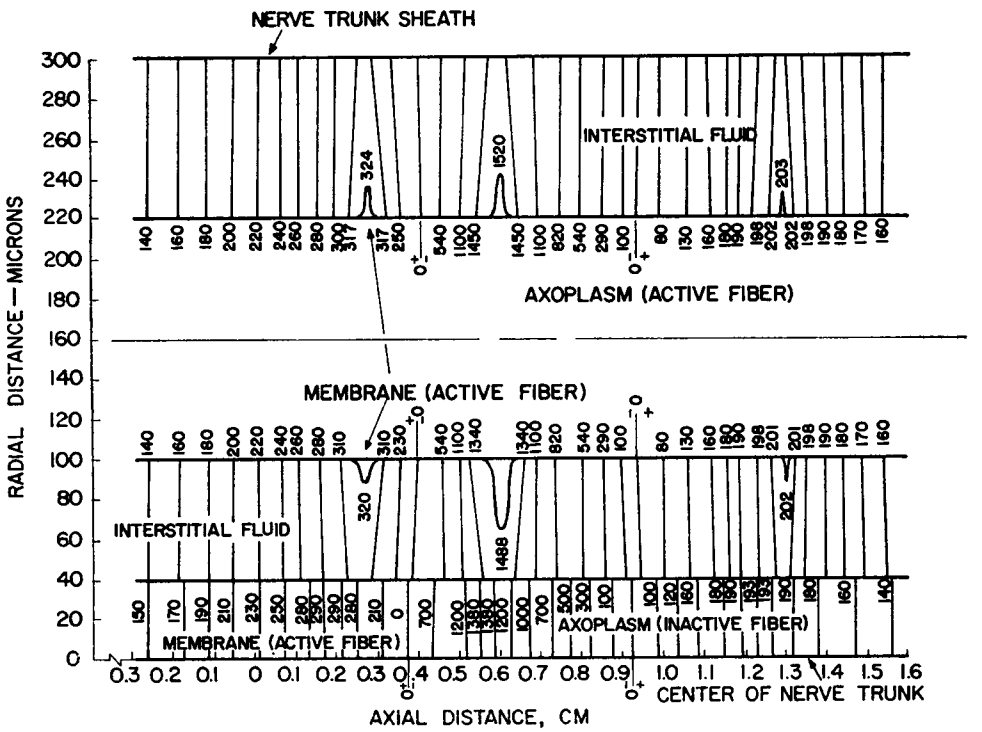

FIGURE 4 Longitudinal aspect of the potential distribution in the interstitial gap region between fibers and in the axoplasmic medium of the inactive fiber ($\theta = 0°$).

observes that the magnitude of induced transmembrane potential is greatest on the side of the inactive fiber nearest the source fiber.

Figs. 4 is a plot of the potential field for $-0.3 < z < 1.6$ cm, $0 < \rho < 100$ μ, and $\theta = 0$; it consequently includes the axoplasmic region of the inactive fiber and the

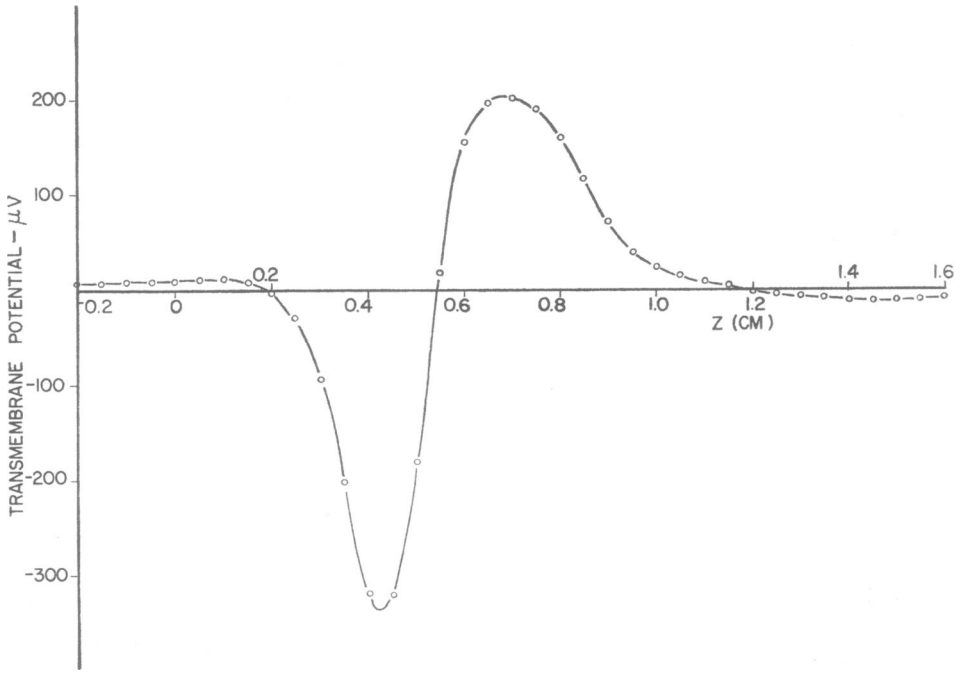

FIGURE 5 Induced transmembrane potential Φ_m as a function of axial distance z ($\theta = 0°$).

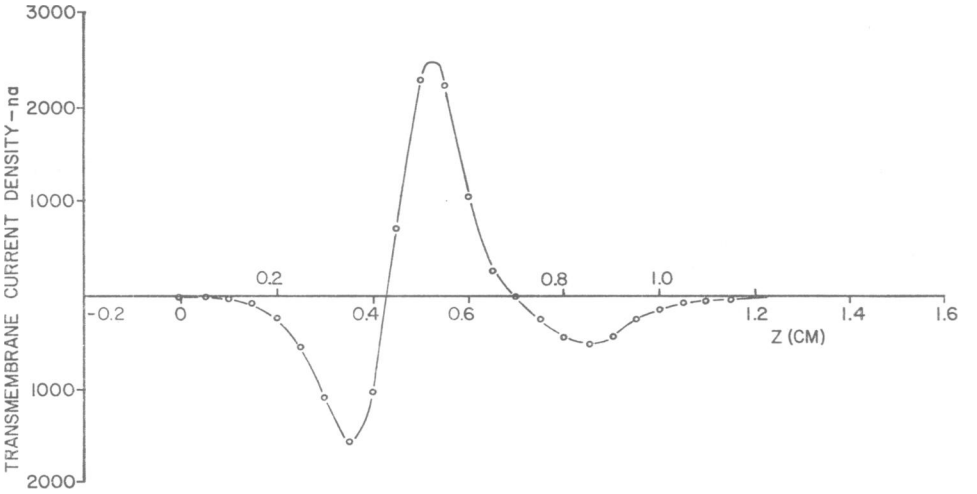

FIGURE 6 Transmembrane current density J_m as a function of axial distance z ($\theta = 0°$).

space between the inactive and active membrane surfaces which lie in the plane $\theta = 0°$. Since lines of current flow lie orthogonal to the isopotential lines of Fig. 4 one can identify three distinct current zones at the source fiber: a central current sink (where current flows inward through the membrane), flanked by two current source

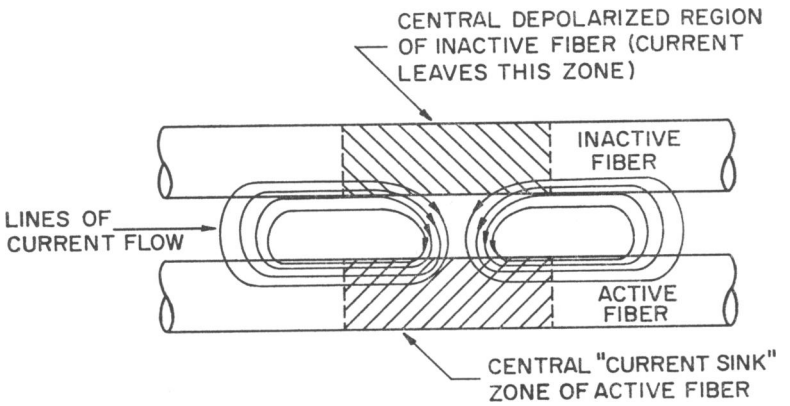

FIGURE 7 Schematic of the idealized action current flow in the fiber interaction problem.

zones (where current flows outward through the membrane). The axoplasmic region of the inactive fiber also contains three such zones which, interestingly, are not in alignment with the interstitial counterpart. This displacement is due to the presence of the electrical capacitance ($\bar{C}_m$) of the inactive fiber membrane, since if $\bar{C}_m$ is set equal to zero and the fields are recomputed, misalignment does not arise. The presence of this misalignment in Fig. 4 makes interpretation somewhat difficult. To facilitate understanding we therefore consider explicitly the transmembrane potential and current density along the inactive fiber. The induced transmembrane potential distribution is easily obtained according to equation 24, and is shown in Fig. 5. The wave form consists of two regions of hyperpolarization flanking a central region of depolarization centered at $z = 0.4$ cm. The early hyperpolarization phase is quite small in amplitude and the wave form could almost be considered to be diphasic in form. The particular waveshape for Φ_{mi} is largely a function of membrane capacitance, as will be shown later.

The transmembrane current density distribution $J_m(z)$ is shown in Fig. 6, and is computed according to equation 23. The wave form for J_m is triphasic in nature, with positive deflections indicating outward current flow. From the information contained in Figs. 4–6, the resultant current field linking the source and inactive fiber may be constructed as shown in Fig. 7.

Effects of Various Model Parameters on the Degree of Fiber Interaction

In this section the effects of various geometrical and electrical parameters on the magnitude of the transmembrane potential induced in the inactive fiber are considered. The parameters of interest are (*a*) the separation distance between fibers, (*b*) ρ_0, the specific resistivity of the interstitial medium (ρ_0 is reciprocally related to σ_0), (*c*) b, the radius of the nerve trunk, and (*d*) ρ_i, the specific resistivity of the axoplasmic medium of the inactive fiber.

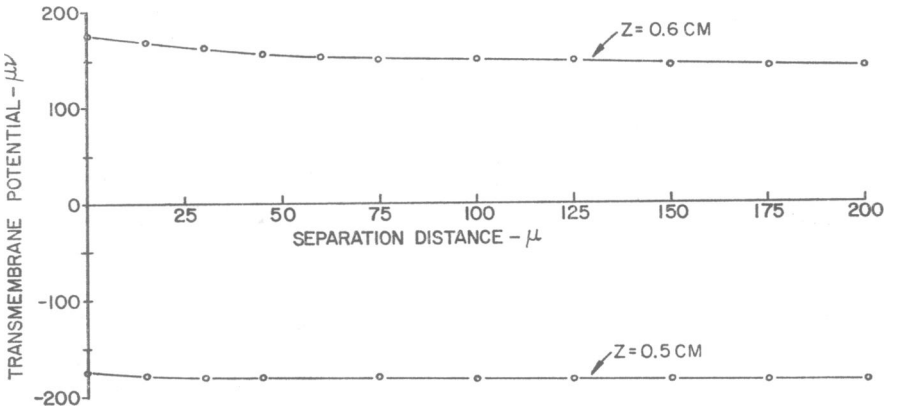

FIGURE 8 Transmembrane potential at $z = 0.5$ cm and $\theta = 0°$ as function of separation distance (S). Nerve trunk radius b is 300 μ.

TABLE III

AXOPLASMIC, INTERSTITIAL, AND TRANSMEMBRANE POTENTIAL FOR VARIOUS VALUES OF S EVALUATED AT $z = 0.5$ AND $z = 0.6$ cm

S	$z = 0.5$ cm			$z = 0.6$ cm		
	Φ^i	Φ^o	Φ_{mi}	Φ^i	Φ^o	Φ^m
0	−1205.861	−1029.502	−176.359	−1356.683	−1633.889	177.307
30	−1196.409	−1016.055	−180.354	−1339.263	−1501.813	162.550
60	−1189.694	−1007.859	−181.835	−1334.847	−1488.960	154.113
100	−1183.636	−1001.219	−182.417	−1330.718	−1481.542	150.824
200	−1177.970	−995.618	−182.352	−1326.703	−1469.779	143.076

Separation Distance and Its Effect on Interaction. The term separation distance (S) refers to the distance between the outer margins of the parallel fibers in the plane $\theta = 0°$. That is, referring to Fig. 1,

$$S = R_s - a - a_s . \tag{37}$$

Intuitively, one might expect that as the fibers are brought progressively closer to one another, the magnitude of the induced transmembrane potential (Φ_{mi}) should be increased. Computation of Φ_{mi} as a function of S at two values of z ($z = 0.5$ and 0.6 cm) and $\theta = 0°$ shows that this is not necessarily true since the curve for $z = 0.5$ cm indicates that Φ_{mi} decreases in magnitude as S decreases; a plot of Φ_{mi} vs. S is given in Fig. 8.

The difference in the behavior of the plots at $z = 0.5$ and $z = 0.6$ cm in Fig. 8 is explained by the fact that the magnitude of interstitial potential is influenced to a greater extent than the axoplasmic potential in response to a change in S. This is clearly shown in Table III.

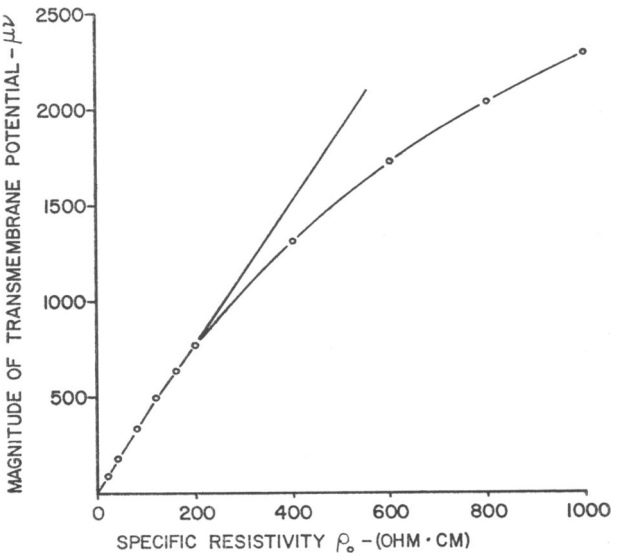

FIGURE 9 Transmembrane potential as a function of the specific resistivity of the interstitial medium for $z = 0.5$ cm and $\theta = 0°$.

TABLE IV

THE SPECIFIC RESISTIVITY OF VARIOUS BIOLOGICAL SUBSTANCES

Substance	Specific resistivity (ρ_0)
	ohm·cm
Ringer fluid	70.0
Sea water	20.0
Human CSF	64.6
Human blood	165.0
Human bone	1800.0
Rabbit cortex	208.0
Human skin	289.0
Intact dog thorax	445.0

CSF = cerebro spinal fluid.

One will observe, however, that the magnitude of change in Φ_{mi}, brought about by decreasing separation distance, is fairly small. This is a little surprising when considering small values of S. For the range $80\,\mu < S < 200\,\mu$ the inactive fiber behaves as if it were in a uniform field, a notion that is roughly consistent with the field pattern seen in Fig. 4. The field uniformity is due to the effect of the nerve trunk sheath.

Specific Resistivity of the Interstitial Medium ρ_0 and Its Effect on the Interaction. (The specific resistivity ρ_0 is reciprocally related to the specific conductivity

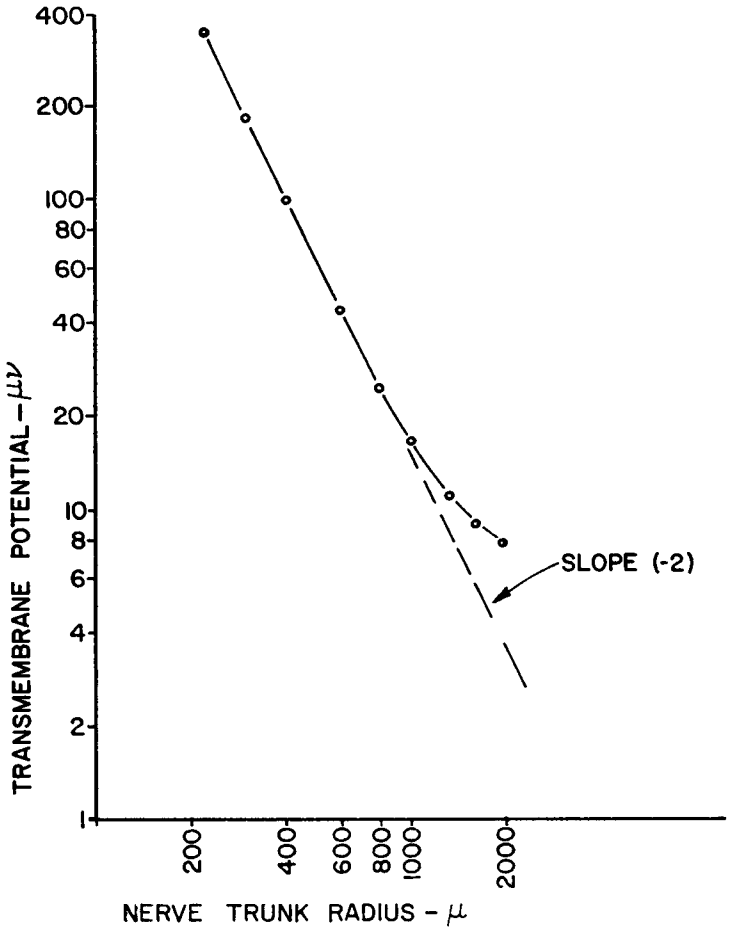

FIGURE 10 Transmembrane potential as a function of nerve trunk radius (b) for $z = 0.5$ cm and $\theta = 0°$.

σ_0.) To investigate the effect of ρ_0 on the magnitude of the induced transmembrane potential, all model parameters with the exception of ρ were held at their typical values and z was set equal to 0.5 cm, $\theta = 0°$, and Φ_{mi} vs. ρ_0 was computed. The result is shown in Fig. 9 and it reveals an approximately linear behavior between transmembrane potential and ρ_0 in the range $0 \leq \rho_0 \leq 200$ ohm·cm. One may also observe from Table IV that the range $20 \leq \rho_0 \leq 200$ ohm·cm might well constitute (in either a physiological or experimental sense) a proper bathing medium for nerve fibers of this type. Thus, for all practical purposes, one could conclude that a linear relationship exists between ρ_0 and Φ_{mi} in the physiologic range of values for ρ_0. The value of ρ_0 used in this study was 40 ohm·cm, a value twice the resistivity of seawater. Considering the fact that the interstitial medium contains a considerable connective

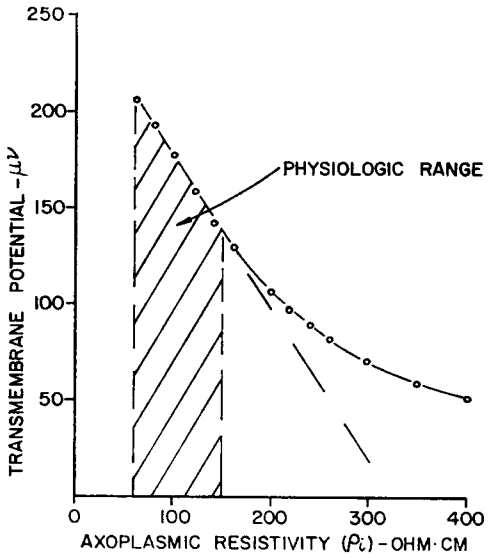

FIGURE 11 Transmembrane potential at $z = 0.5$ cm and $\theta = 0°$, as a function of ρ_i, the specific resistivity of the inactive fiber.

tissue component, as well as other inactive nerve fibers and blood vessels, an average value of 40 ohm·cm is probably much lower than what might actually be measured *in situ*. Consequently, the computed values of transmembrane potential given in previous figures may be low; if ρ_0 were say 160 ohm·cm then Φ_{mi} would increase by a factor of 4.

Nerve Trunk Radius and Its Effect on Fiber Interaction. One of the most important model parameters insofar as interaction effects are concerned, is the radius (b) of the nerve trunk. Fig. 10 indicates that as the radius is increased, the magnitude of Φ_m rapidly decreases such that for radii greater than 1300 μ, transmembrane potential is essentially uninfluenced by the presence of the epineural sheath. Such a situation corresponds to the condition of the interaction of two fibers in an infinite volume conductor, and, as one can see from Fig. 10, the magnitude of Φ_{mi} becomes quite small.

The Effect of Variation in the Specific Resistivity of the Axoplasmic Region of the Inactive Fiber (Fig. 11). We note that Φ_{mi} increases for diminishing resistance. If the interstitial field is seen as the driving force, a greater fraction of potential appears across the membrane as the internal resistance per unit length diminishes. Over the physiologic range this effect is of secondary importance as revealed in Fig. 11.

DISCUSSION OF RESULTS

The aforementioned results are consistent with the following simple model. The active fiber is thought of as a constant voltage generator whose internal resistance is proportional to its axoplasmic resistance per unit length. The electric field in the

interstitial region must then be proportional to the *effective* axial resistance per unit length of the interstitial space. For trunk radii that are not too large compared with that of the active fiber the effective interstitial axial resistance per unit length will be inversely proportional to the trunk radius. (In the absence of an inactive fiber such a relationship has been demonstrated in Clark and Plonsey [1968] Fig. 13.) In the present context it is not unreasonable for the transmembrane potential of the inactive fiber to be proportional to the field along its surface. As a consequence one expects Φ_{mi} to be inversely proportional to the square of the nerve trunk radius for "small" radii. This is indeed the case as revealed in Fig. 10, for nerve trunk radii less than 500 μ. The linear dependence of Φ_{mi} on ρ_0 is explained by the same mechanism. While the two-fiber geometry represents a very simple example, it lends insight into the general nature of fiber interaction both within the nerve trunk and in the infinite medium. Through variation of various model parameters, it has been found that the cross-sectional area of the trunk and the specific resistivity of the intersititial medium are of particular importance to fiber interaction (Figs. 10 and 11), as well as the general magnitude of potential (Φ^e) within the interstitial medium. With regard to the latter, the cross-sectional area of the trunk is particularly important, since it affects not only the magnitude of Φ^e, but also its distribution with axial distance z. In general, as nerve trunk radius increases, the spatial distribution of potential becomes less uniform (Fig. 4), and interstitial potential magnitude decreases rapidly (Clark and Plonsey, 1968). The value of ρ_0 also considerably influences both the magnitude of induced transmembrane potential (Fig. 9) and interstitial potential (Clark and Plonsey, 1968). The magnitude and distribution of the interstitial potential is quite important in that it represents the impressed field in which other fibers within the trunk lie. The value of ρ_0 used in this study (40 ohm·cm) is considered to be a very conservative value with respect to evaluating interaction effects. If a value of 160 ohm·cm had been used Φ_{mi} would have increased by a factor of approximately 4 (Fig. 9). The separation between fibers is another factor influencing the magnitude of Φ_{mi}. Fig. 8 indicates, however, that it is of much less importance than either cross-sectional area or ρ_0. Studies of the effect of changes in membrane resistance ($\bar{r}_m$) and capacitance ($\bar{C}_m$) on transmembrane potential indicate that these parameters are also of much less importance than either cross-sectional area or ρ_0 (Clark, 1967).

The results of this work agree essentially with the experimental findings of Katz and Schmitt (1940, 1942). The real significance of this work, however, does not lie only in the statement that such a theoretical model can produce data that is consistent with experimental fact. Rather, with minimal input data of a measurable nature (wave shape of the action potential, conduction velocity, typical values for the conductivities of the media, membrane resistance and capacitance, separation distance), this model provides a quantitative description of such things as (*a*) the potential distributions in the bathing medium and axoplasmic media of the active and

inactive nerve fibers, and (*b*) the transmembrane potential and current density distributions. Some of these quantities are of a measurable nature, while others are not. For example, potential changes in the inactive fiber could be monitored using present-day microelectrode techniques. On the other hand, measuring interstitial potential or transmembrane current density would certainly involve considerable measurement difficulty. Yet the behavior of all such quantities is of importance to the electrophysiologist attempting to understand and model the nerve trunk problem.

APPENDIX

The following equations represent the derived expressions for potential in the media of interest:

$$\Phi^i(\rho, \theta, z) = \frac{2}{a}\cos n\theta \int_0^\infty \frac{[A_n^{(1)}(y)\beta^{(1)}(y) + A_n^{(2)}(y)\beta^{(2)}(y)]}{DA_n(y)} I_n(y\rho/a)\, dy \qquad (A1)$$

$$\Phi^o(\rho, \theta, z) = \frac{2}{a}\cos n\theta \int_0^\infty \left[\left[\left(K_n\left(\frac{yR_s}{a}\right) + (\gamma_n^b B_n^{(1)}(y)/DD_n(y)\right) I_n\left(\frac{y\rho}{a}\right) + C_n^{(1)}(y)K_n\left(\frac{y\rho}{a}\right)\right]\beta^{(1)}(y) + \left[((\gamma_n^b B_n^{(2)})/DD_n(y))I_n\left(\frac{y\rho}{a}\right) + C_n^{(2)}(y)K_n\left(\frac{y\rho}{a}\right)\right]\beta^{(2)}(y)\right] dy \quad \text{for} \quad \rho < R_s \qquad (A2)$$

$$\Phi^o(\rho, \theta, z) = \frac{2}{a}\cos n\theta \int_0^\infty \left[\left[\left(\gamma_n^b(y)B_n^{(1)}(y)I_n\left(\frac{y\rho}{a}\right)\right)\Big/ DD_n(y) + \left(I_n\left(\frac{yR_s}{a}\right) + C_n^{(1)}(y)\right)K_n\left(\frac{y\rho}{a}\right)\right]\beta^{(1)}(y) + \left[\left(\gamma_n^b(y)B_n^{(2)}(y)I_n\left(\frac{y\rho}{a}\right)\right)\Big/ DD_n(y) + C_n^{(2)}(y)K_n\left(\frac{y\rho}{a}\right)\right]\beta^{(2)}(y)\right] dy \quad \text{for} \quad \rho > R_s \qquad (A3)$$

where

$$y = ka \qquad (A4)$$

$$A_n^{(1)}(y) = [\bar{\sigma}_m EZ_0 + (\bar{Y}_m)^2 I_n(y) - \bar{Y}_m \sigma_i I_n'(y) EZ_4 B^{(2)}(y)] \qquad (A5)$$

$$A_n^{(2)}(y) = -[(\bar{\sigma}_m EZ_0 + (\bar{Y}_m)^2 I_n(y))EZ_4 B_n^{(2)}(y) + \sigma_i \bar{Y}_m I_n'(y)(EZ_2 DD_n(y) - EZ_4 B^{(1)}(y))] \qquad (A6)$$

$$DD_n(y) = [\sigma_0 EZ_0 EZ_3 + \sigma_i \bar{\sigma}_m I_n'(y) EZ_4]^2 + \sigma_0 I_n(y) EZ_3 + \sigma_i I_n'(y) EZ_4]^2 \bar{Y}_m^2 \qquad (A7)$$

$$DA_n(y) = [(\sigma_i I_n'(y) + \bar{\sigma}_m I_n(y))^2 + (\bar{Y}_m I_n(y))^2] DD_n(y) \quad (A\ 8)$$

$$\beta^{(1)}(y) = P_n(y) \sum_{i=1}^{3} e^{-y^2/4a^2 B_i^2} \cos y \frac{(z - C_i)}{a} \quad (A\ 9)$$

$$\beta_n^{(2)}(y) = P_n(y) \sum_{i=1}^{3} e^{-y^2/4a^2 B_i^2} \sin y \frac{(z - C_i)}{a} \quad (A\ 10)$$

$$P_n(y) = (2 - \delta_n^o)/(2\sqrt{\pi}\alpha(y) K_0(ya_e/a)) \quad (A\ 11)$$

$$\alpha(y) = -\left[\frac{\sigma_0}{\sigma_{is}} \frac{K_1(ya_e/a) I_0(ya_e/a)}{K_0(ya_e/a) I_1(ya_e/a)} + 1\right] \quad (A\ 12)$$

$$\gamma_n^b(y) = \left[\frac{\sigma_0 \sigma_e}{\bar{\sigma}_{sh}} K_n'\left(\frac{yb}{a}\right) + (\sigma_e - \sigma_0) K_n\left(\frac{yb}{a}\right)\right]\left[K_n'\left(\frac{yb}{a}\right) \Big/ \bar{\sigma}_{sh}\right] \quad (A\ 13)$$

$$\alpha_n^b(y) = \frac{1}{\bar{\sigma}_{sh}}\left[\frac{\sigma_0 \sigma_e}{\bar{\sigma}_{sh}} I_n'\left(\frac{yb}{a}\right) K'n\left(\frac{yb}{a}\right) + \sigma_e I_n\left(\frac{yb}{a}\right) K_n'\left(\frac{yb}{a}\right) - \sigma_0 I_n'\left(\frac{yb}{a}\right) K_n\left(\frac{yb}{a}\right)\right] \quad (A\ 14)$$

$$EZ_0 = \sigma_i I_n'(y) + \bar{\sigma}_m I_n(y) \quad (A\ 15)$$

$$EZ_1 = K_n'(y) I_n\left(\frac{yR_s}{a}\right) - I_n'(y) K_n\left(\frac{yR_s}{a}\right) \quad (A\ 16)$$

$$EZ_2 = I_n(y) K_n\left(\frac{yR_s}{a}\right) - K_n(y) I_n\left(\frac{yR_s}{a}\right) \quad (A\ 17)$$

$$EZ_3 = I_n'(y)\gamma_n^b(y) - K_n'(y)\alpha_n^b(y) \quad (A\ 18)$$

$$EZ_4 = \alpha_n^b(y) K_n(y) - \gamma_n^b(y) I_n(y) \quad (A\ 19)$$

$$C_n^{(1)}(y) = -\left[I_n\left(\frac{yR_s}{a}\right) + \alpha_n^b(y) B_n^{(1)}(y)/DD_n(y)\right] \quad (A\ 20)$$

$$C_n^{(2)}(y) = -[\alpha_n^b(y) B_n^{(2)}(y)]/DD_n(y) \quad (A\ 21)$$

$$BB_1(y) = \sigma_0 EZ_0 EZ_1 + \sigma_i \bar{\sigma}_m I_n'(y) EZ_2 \quad (A\ 22)$$

$$BB_2(y) = \bar{Y}_m[\sigma_0 I_n(y) EZ_1 + \sigma_i I_n'(y) EZ_2] \quad (A\ 23)$$

$$DN_1(y) = \sigma_0 EZ_0 EZ_3 + \sigma_i \bar{\sigma}_m I_n'(y) EZ_4 \quad (A\ 24)$$

$$DN_2(y) = \bar{Y}_m(\sigma_0 I_n(y)EZ_3 + \sigma_i I_n'(y)EZ_4) \quad (A\ 25)$$

$$B_n^{(1)}(y) = BB_1(y)DN_1 + BB_2(y)DN_2(y) \quad (A\ 26)$$

$$B_n^{(2)}(y) = BB_1(y)DN_2(y) - BB_2(y)DN_1(y) \quad (A\ 27)$$

$$\bar{Y}_m = y\nu\bar{C}_m/a \quad (A\ 28)$$

The prime notation associated with the modified Bessel function represents the derivative of the Bessel function. For example,

$$I_n'(y) = y/a\left(\frac{n}{y} I_n(y) + I_{n+1}(y)\right) \quad (A\ 29)$$

$$K_n'(y) = y/a\left(\frac{n}{y} K_n(y) - K_{n+1}(y)\right). \quad (A\ 30)$$

The expression for transmembrane current density $J_m(\theta_1 Z)$ is:

$$J_m(\theta, Z) = \frac{-2\sigma_0}{a} \cos n\theta \int_0^\infty \Bigg[\Bigg[\Bigg(K_n\left(\frac{yR_e}{a}\right) + (\gamma_n^b(y)B_n^{(1)}(y))/DD_n(y)\Bigg)I_n'(y) + C_n^{(1)}(y)K_n'(y)\Bigg] B^{(1)}(y) + [(\gamma_n^b(y)B_n^{(2)}(y)I_n'(y)/DD_n(y) + C_n^{(2)}(y)K_n'(y)]B^{(2)}(y)\Bigg] dy. \quad (A\ 31)$$

This research was supported by Public Health Service Grant HE 10417 and the Rice Health Science Advancement Award 5-S04-FR-06136-01 from the General Research Branch, National Institutes of Health.

Received for publication 19 August 1969.

REFERENCES

ARVANITAKI, A. 1942. *J. Neurophysiol.* **5**:89.
BURES, J., M. PETRAN, and J. ZACHAR. 1967. Electrophysiological Methods in Biological Research. Academic Press Inc., New York. 339–342.
CLARK, J. W. 1967. Ph.D. Thesis. Case Western Reserve University, Cleveland.
CLARK, J. W., and R. PLONSEY. 1966. *Biophys. J.* **6**:95.
CLARK, J. W., and R. PLONSEY. 1968. *Biophys. J.* **8**:842.
ESPLIN, D. 1962. *J. Neurphysiol.* **25**:805.
GRANIT, R., L. LEKSELL, and C. R. SKOGLUND. 1944. *Brain.* **67**:125.
GRUNDFEST, H., and J. MAGNES. 1951. *Amer. J. Physiol.* **164**:502.
KATZ, B., and O. SCHMITT. 1940. *J. Physiol.* **97**:471.
KATZ, B., and O. SCHMITT. 1942. *J. Physiol.* **100**:369.
KONISHI, K. 1955. *Jap. J. Physiol.* **5**:101.
MARAZZI, A., and R. LORENTE DE NÓ. 1944. *J. Neurophysiol.* **7**:83.
WATANABE, A., and H. GRUNDFEST. 1961. *J. Gen. Physiol.* **45**:267.